Alignment of carbon nanotubes in a polymer matrix by mechanical stretching

L. Jin,[a] C. Bower,[b] and O. Zhou[a),c)]
University of North Carolina at Chapel Hill, Chapel Hill, North Carolina 27599

(Received 7 April 1998; accepted for publication 29 June 1998)

We report a method to fabricate polymer-based composites with aligned carbon nanotubes, and a procedure to determine the nanotube orientation and the degree of alignment. The composites were fabricated by casting a suspension of carbon nanotubes in a solution of a thermoplastic polymer and chloroform. They were uniaxially stretched at 100 °C and were found to remain elongated after removal of the load at room temperature. The orientation and the degree of alignment were determined by x-ray diffraction. The dispersion and the alignment of the nanotubes were also studied by transmission electron microscopy. © *1998 American Institute of Physics.* [S0003-6951(98)00435-5]

Carbon nanotubes (CNTs) can now be produced in high yield and reasonable quality by several techniques.[1,2] These one-dimensional (1D) nanostructures are shown to have superior mechanical and novel electronic properties, which are not only sensitive to their diameter and chirality but are also highly anisotropic. Although tremendous progress has been made towards understanding the properties of individual CNTs using local probes such as the scanning tunneling microscope[3,4] and atomic force microscope,[5,6] investigating the bulk anisotropic properties and utilizing them for practical applications have been hindered by the lack of materials with controllable degree of alignment. CNTs produced by the arc-discharge,[1] chemical vapor deposition,[7] and laser ablation[8] methods are all randomly oriented.

There are several previous reports on fabricating aligned nanotubes. Ajayan *et al.*[9] fabricated a composite with CNTs randomly dispersed inside an epoxy matrix and found that slicing the composite caused partial alignment of the nanotubes on the *cut surface*. de Heer *et al.*[10] fabricated aligned nanotube films by drawing a nanotube suspension through a micropore filter. Wang *et al.*[11] synthesized multiwalled carbon nanotubes by arc discharge and observed, by electron microscopy, arrays of parallel bundles. Terrones *et al.*[12] produced aligned multiwalled nanotubes on a patterned substrate by pyrolysis. In this letter, we present a simple method to fabricate polymer-based composite with aligned nanotubes and a procedure to determine the nanotube orientation and the degree of alignment.

Multiwalled carbon nanotubes (MWNTs) synthesized by the arc-discharge method[2] were used in this study. The volume fraction of the impurity multishell nanoparticles was estimated to be ~30% by transmission electron microscopy (TEM). After screening several polymers and solvents based on their solubility and mechanical properties, a thermoplastic polymer, polyhydroxyaminoether (PHAE, supplied by the Dow Chemical Co.), was chosen. The MWNTs were ground to fine powders and sonicated in chloroform ($CHCl_3$) for 1 h at room temperature. PHAE was then dissolved into the nanotube/chloroform suspension. After another hour of sonication, the suspension was transferred into a Teflon mold and air dried in a fume hood overnight. A black thin film was formed which was peeled off. Pure PHAE and composite films with nanotube weight fraction up to 50% were made and cut into $\sim 5 \times 3$ mm strips. The strips were mechanically stretched by applying a constant load at 95–100 °C. Different loads were used. Under optimum conditions, most composites can be stretched up to 500% (final length L over initial length L_0) without fracture. After the desired stretching ratio was obtained, the sample was first cooled down to room temperature then the load released.

X-ray diffraction patterns were collected from both the unstretched and stretched samples (after the load was released) at room temperature. Data were collected using a 1.5 kW Cu $K\alpha$ source, HOPG(002) monochromator, and a two-dimensional (2D) imaging plate detector in the transmission mode. Multiwalled nanotubes and nanoparticles have been studied previously by x-ray diffraction techniques.[13,14] The diffraction spectrum is dominated by a strong Bragg peak centered around 3.4 Å, which corresponds to the intershell spacing within the nanotubes and nanoparticles [referred to as the (002) peak hereafter]. The slightly larger d spacing (compared to that of graphite) is related to the stacking disorder in these nanostructures. When the nanotubes are randomly oriented inside the polymer matrix, a powder diffraction ring with a d spacing of ~3.4 Å and a uniform intensity distribution is expected, as illustrated in Fig. 1. If the nanotubes have a preferred orientation, the Bragg intensities will be concentrated at two spots at the intersections of the plane defined by $\mathbf{K}_i$ (incident x-ray beam) and $\mathbf{Q}_{002}$ (reciprocal space vector), and the powder ring.

A typical 2D x-ray diffraction pattern of an as-cast composite film collected in the transmission mode with $\mathbf{K}_i$ perpendicular to the stretching axis is shown in Fig. 2(a). The narrow ring marked by the arrow is the (002) Bragg peak of the nanotubes and nanoparticles. The data were processed and are plotted as intensity versus 2θ and azimuth angle ϕ in the rectangular panel. As discussed above, the (002) Bragg peak was found to be centered around 26.1° in 2θ ($d = 3.41$ Å) and is essentially a constant with respect to ϕ,

[a)]Curriculum of Applied and Materials Science.
[b)]Department of Physics and Astronomy.
[c)]Author to whom correspondence should be addressed.

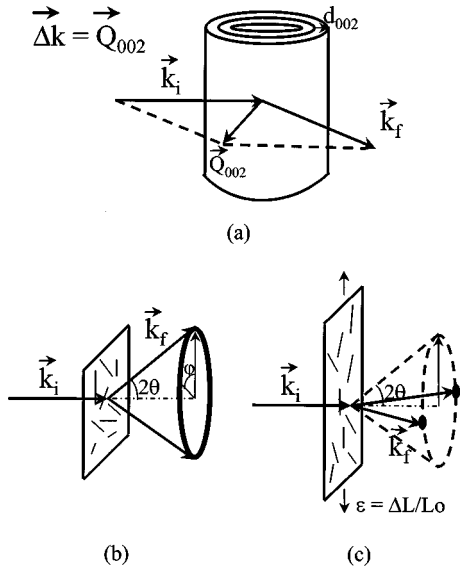

FIG. 1. Schematics of the x-ray diffraction geometry. (a) A multiwalled carbon nanotube (NT). Because of the Bragg law, the scattered x-ray beam ($\mathbf{K}_f$), the incident beam ($\mathbf{K}_i$), and the intershell reciprocal space vector $\mathbf{Q}_{002}$ are on the same plane perpendicular to the nanotube longitudinal axis. (b) In an as-cast composite film the NTs are expected to be randomly oriented and will show a powder diffraction ring with intensity uniformly distributed azimuthally along the circumference. (c) In a stretched film, the NTs are likely to have a preferred orientation with their longitudinal axes parallel to the strain direction ($\boldsymbol{\epsilon}$). As a result, the Bragg intensity will be concentrated at two spots at $\phi = 90°$ and 270°, respectively.

from 0° to 360° (along the circumference of the diffraction ring).

The x-ray diffraction pattern of a stretched ($L/L_0 = 330\%$) composite film (50 wt % of raw carbon nanotube

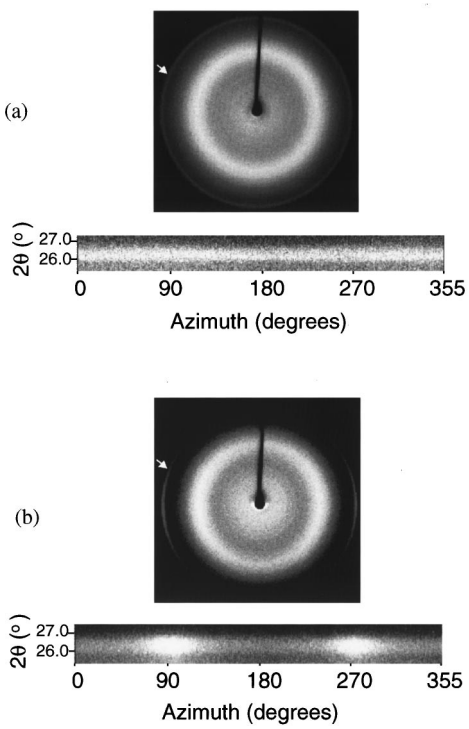

FIG. 2. 2D x-ray diffraction patterns obtained from: (a) an as-cast MWNT/polymer composite; and (b) a composite composed of 50 wt % CNTs after being stretched by 330% (L/L_0). The narrow ring (a) and arcs (b) pointed by the arrows are the (002) peaks of the multiwalled nanotubes (and nanoparticles). The rectangular panels show the intensity vs 2θ and azimuth (ϕ) plots obtained by unwrapping the circular diffraction rings and renormalizing the intensity.

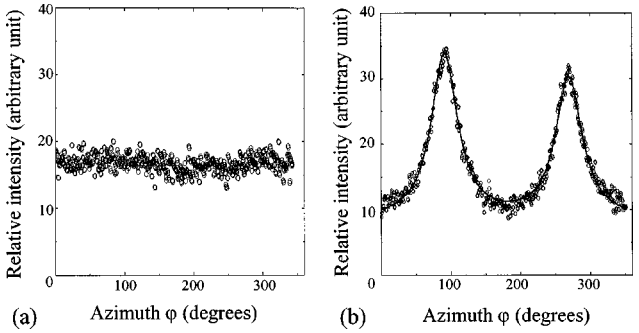

FIG. 3. Integrated x-ray intensity (integrated along the 2θ axis) vs the azimuth for an as-cast film (a), and a 50 wt % CNT composite after being stretched by 330% (b). The solid line is a fit to the data by two Lorentzian functions and a constant background.

materials) is shown in Fig. 2(b). The (002) Bragg intensity is now concentrated at two spots centered at $\phi \approx 90°$ and 270°. The change in the diffraction pattern from a uniform powder ring before stretching to two spots indicates that the nanotubes in the stretched composite film were aligned. The location of the Bragg spots with respect to $\mathbf{K}_i$ shows that the nanotubes were aligned with their longitudinal axes parallel to $\boldsymbol{\epsilon}$.

In addition to the two strong Bragg spots, a weak (002) intensity ring was also observed. Two sources contribute to this intensity: the nanotubes that were randomly oriented and the nanoparticles in the starting materials. Because of their quasispherical geometry, the (002) diffraction intensities from the nanoparticles should be uniformly distributed along the circumference of the powder ring before and after stretching. The exact volume ratio of the nanoparticles is not known and is roughly estimated to be ~30%.

To estimate the fraction of the nanotubes that was aligned and the degree of alignment, the x-ray data were analyzed in two steps. First, the 2D intensity data (intensity I versus 2θ and ϕ) were integrated in the ϕ direction, and plotted as I versus 2θ. In addition to the (002) peak, a broad hump centered around 18° 2θ was observed, which is assigned to the diffuse scattering from the polymer matrix. The (002) Bragg peak was fitted to a Gaussian function plus a polynominal background.

Next, the 2D intensity data were integrated along the 2θ axis and plotted as I versus azimuth ϕ after subtracting out the background intensity in Figs. 3(a) and 3(b) for the as-cast and stretched materials, respectively. As expected, the diffraction intensity from the as-cast sample is essentially a constant over the whole ϕ range, indicating random orientation of the nanotubes. The spectrum in Fig. 3(b) was fitted using two Lorentzian functions with the same width and a constant background. The fitted intensity is plotted in Fig. 3(b) as a solid line. The two peaks were found to be centered at $\phi = 90.9°$ and 270.1°, respectively, and are 179.2° apart. The fitted full width at half maximum of the two Lorentzian functions is 46.4°, which means that the aligned nanotubes have a mosaic angle of ±23.2° around the stretching axis.

The amount of aligned nanotubes is proportional to the total integrated intensity of the two Lorentzian peaks in Fig. 3(b). The total amount of randomly dispersed nanotubes and nanoparticles scales with the constant intensity. Assuming the quasispherical nanoparticles constitute ~30% of the raw

nanotube material, the data imply that 58% of the nanotubes in the sample with 330% elongation were partially aligned along the stress direction, with a mosaic angle of $\pm 23°$.

Similar analyses performed on composites with different stretching ratios showed that the fraction of the nanotubes aligned decreases, and the mosaic angle increases, with decreasing stretching ratio. For example, in a composite with 50 wt % of MWNTs, 28% of the nanotubes were aligned with a mosaic of ± 30.5 at $L/L_0 = 250\%$. At the same L/L_0 ratio, composites with 20 wt % of CNTs were found to have a narrower mosaic. The difference is attributed to the effect of nanotube concentration on their mobility. For thick samples, it is difficult to stretch the materials to the same maximum elongation obtained in the thin samples. Necking and fracture occur at lower strains. However, the degree of alignment is the same at a given stretching ratio, regardless of the sample thickness.

Preliminary results suggest that the rigidity and aspect ratio of the nanotubes play important roles in their ease and degree of alignment. For example, when subjected to similar stretching ratios, no significant alignment was obtained for composites composed of single-walled nanotube bundles, which are known to be more flexible and have much higher aspect ratios than the multiwalled nanotubes.

The dispersion and alignment of the carbon nanotubes in the polymer matrix were examined by TEM. The composite samples were cut into ~90 nm thick membranes using microtomy with a diamond blade. The nanotubes and the impurity nanoparticles were found to be dispersed in the matrix without significant aggregation and were wetted by the polymer. Figure 4(a) shows fiber pull-out in an internal fracture surface of a composite after being sliced parallel to the stretching direction. The nanotubes were found to be aligned with their longitudinal axes parallel to the stretching direction, consistent with the conclusion from x-ray analyses. In some areas, nanotubes were found to bridge the microvoids (or microcracks) in the matrix and presumably enhanced the strength of the composite. Figure 4(b) shows the cross-sectional view of the composite perpendicular to the stretching direction. Here, the cross sections of the nanotubes and nanoparticles were observed. The fact that slicing did not realign the nanotubes parallel to the cutting direction, as observed in the epoxy/nanotube composite,[9] indicates strong bonding between the nanotubes and the polymer matrix.

In summary, the results presented in this brief communication demonstrate a simple method to fabricate nanotube/polymer composites and mechanically align the nanotubes inside the polymer matrix. By controlling the stretching ratio, the degree of alignment can be varied, which is critical for elucidating the intrinsic anisotropic properties of the nanotubes that are not obscured by the matrix material. The method described here should be applicable to other 1D nanostructures.

The authors thank H. Hiura for providing the multiwalled nanotubes and J. White for supplying the PHAE polymer used in this study, D. Taylor and E. Samulski for discussions, and W. Ambrose for assistance in TEM measurements. O.Z. acknowledges support from the NSF (INT-9603262 and ECS-9700677) and the ONR (through a MURI program, N00014-98-1-0597).

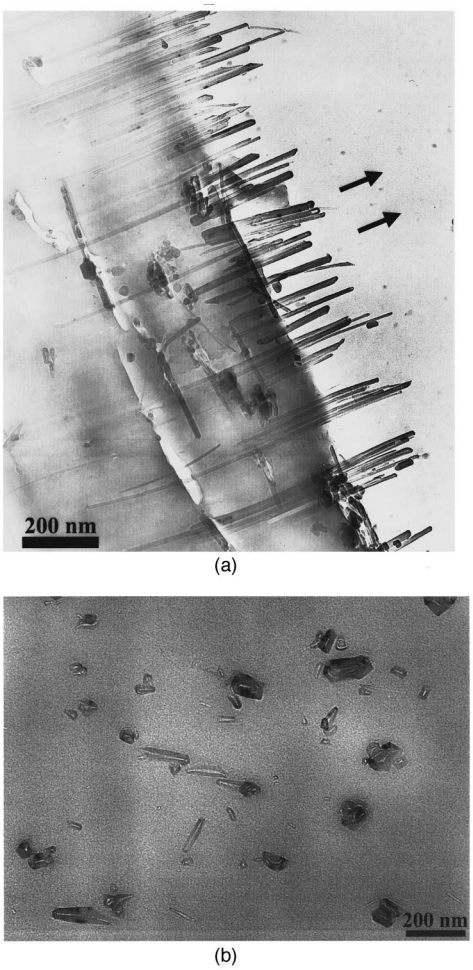

FIG. 4. (a) TEM image of an internal fracture surface of a composite after being sliced parallel to the stretching direction by a microtome. The sample thickness is about 90 nm. It shows fiber pull-out. The nanotubes are aligned parallel to the stretching direction. In some areas, nanotubes bridge the microvoids (or microcracks) in the matrix and presumably enhance the strength of the composite. (b) Cross-sectional view of the same composite sliced perpendicular to the stretching direction. Here, the cross sections of the nanotubes and nanoparticles were observed.

[1] S. Iijima, Nature (London) **354**, 56 (1991).
[2] T. W. Ebbesen and P. M. Ajayan, Nature (London) **358**, 16 (1992).
[3] J. W. G. Wildöer, L. C. Venema, A. G. Rinzler, R. E. Smalley, and C. Dekker, Nature (London) **391**, 59 (1998).
[4] T. W. Odom, J. L. Huang, P. Kim, and C. M. Lieber, Nature (London) **391**, 62 (1998).
[5] E. W. Wong, P. E. Sheehan, and C. M. Lieber, Science **277**, 1971 (1997).
[6] M. R. Falvo, G. J. Clary, R. M. Taylor II, V. Chi, F. R. Brooks, Jr., S. Washburn, and R. Superfine, Nature (London) **389**, 582 (1997).
[7] M. Endo, K. Takeuchi, S. Igarashi, K. Kobori, M. Shiraishi, and H. W. Kroto, J. Phys. Chem. Solids **54**, 1841 (1993).
[8] A. Thess, R. Lee, P. Nikdaev, H. Dai, P. Petit, J. Robert, C. Xu, Y. H. Lee, S. G. Kim, A. G. Rinzler, D. T. Colbert, G. E. Scuseria, D. Tomanek, J. E. Fischer, and R. E. Smalley, Science **273**, 483 (1996).
[9] P. M. Ajayan, O. Stephan, C. Colliex, and D. Trauth, Science **265**, 1212 (1994).
[10] W. A. de Heer, A. Châtelain, and D. Ugarte, Science **270**, 1179 (1995).
[11] X. K. Wang, X. W. Lin, V. P. Dravid, J. B. Ketterson, and R. P. H. Chang, Appl. Phys. Lett. **62**, 1881 (1993).
[12] M. Terrones, N. Grobert, J. Olivares, J. P. Zhang, H. Terrones, K. Kordatos, W. K. Hsu, J. P. Hare, P. D. Townsend, K. Prassides, A. K. Cheetham, H. W. Kroto, and D. R. M. Walton, Nature (London) **388**, 52 (1997).
[13] O. Zhou, R. M. Fleming, D. W. Murphy, C. T. Chen, R. C. Haddon, A. P. Ramirez, and S. H. Glarum, Science **263**, 1744 (1994).
[14] D. Reznik, C. H. Olk, D. A. Neumann, and J. R. D. Copley, Phys. Rev. B **52**, 116 (1995).